$RuHX(CO)(PR_3)_2$: Can ν_{CO} Be a Probe for the Nature of the Ru–X Bond?

Jason T. Poulton,[†] Michael P. Sigalas,[‡,§] Kirsten Folting,[†] William E. Streib,[†] Odile Eisenstein,*[,§] and Kenneth G. Caulton*[,†]

Department of Chemistry and the Molecular Structure Center, Indiana University, Bloomington, Indiana 47405, and Laboratoire de Chimie Théorique, Bât. 490, Université de Paris-Sud, 91405 Orsay, France

Received May 19, 1993[⊗]

The relative electron-donating ability of X in the new five-coordinate $RuHX(CO)(P^tBu_2Me)_2$ (X = I, Br, Cl, F, OPh, OH, OCH_2CF_3, OEt, $OCPh_3$, $OB(Mesityl)_2$, $OSiR_3$, NHPh, SPh, C_2Ph) has been evaluated based on the CO stretching frequency. In all cases, the CO frequency is lower than that of the free CO and the reduction increases in the order I < Br < Cl < F < alkoxide, with the ethoxide inducing the largest shift. NHPh behaves as OPh and SPh appears at a higher frequency than OPh. Similar measurements have been conducted on the six-coordinate pyridine adducts and a similar ranking of CO frequencies is obtained, but all frequencies are shifted lower. Hydride is the weakest of all donors. There can be no conventional (two-center) Ru–X π-bonding in these pyridine adducts because the Ru(d)/X(p_π) interactions are two-orbital/four-electron ones and thus are net destabilizing. However, the CO π^* orbitals interact to stabilize the Ru–X π^* orbital, thereby retaining some degree of net Ru–X π bonding. The structure of $RuH(OSiPh_3)(CO)(P^tBu_2Me)_2$ is shown to be square pyramidal with H at the apical site of the pyramid and the siloxy group *trans* to CO. EHT and core-potential *ab initio* calculations (full optimization at the HF and partial optimization at the MP2 level) have been performed to determine the structure of $RuHX(CO)(PH_3)_2$ (X = F, Cl, OH, OCH_3, $OSiH_3$ with d orbitals on the Si atom). The square pyramid is preferred for all X. This structure permits optimal push–pull effects between the π-donating X group and the π^* of CO. The CO frequency has been calculated at the MP2 level, and the ranking is identical to the experimental ones. π effects are shown to be larger for alkoxy than for halide, but the variation in π-effects alone is not sufficient to account for the ranking of the CO frequencies down a column of the periodic table; the σ effect is also involved. In particular, it is shown that strongly ionic Ru–X bonds lead to lower CO frequency. This last effect causes large changes in the ^{19}F chemical shift for $RuH(F)(CO)(P^tBu_2Me)_2$ species upon adding a sixth ligand to Ru. It also causes strong hydrogen bonding of fluoride to added alcohol. In spite of Ru/X multiple bonding in the five-coordinate species, they are Lewis acidic toward amines and phosphines. Crystal data for $RuH(OSiPh_3)(CO)(P^tBu_2Me)_2$ at −160 °C: a = 11.263(1) Å, b = 31.713(4) Å, c = 22.311(3) Å, and β = 100.07(0)° with Z = 4 in space group $P2_1/n$.

Introduction

Following the report of Halpern[1a] on the synthesis and reactivity of $Ir(H)_2(OR_f)P_2$ (R_f = CH_2CF_3, P = phosphine), we have pursued[1b] the idea that potential π-donor ligands (those bearing two or more lone pairs in their anionic form) can provide temporary stabilization (by X→M π-donation) to a late transition metal compound. It was hoped that such X→M multiple bonding would revert to a single bond either before or during the approach of a nucleophile (eq 1) thereby allowing ready coordination without

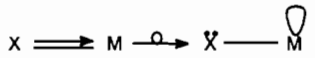

(1)

the need for the thermal or photochemical activation which characterizes saturated compounds like $M(CO)_6$ (M = Cr, Mo, W), $Fe(CO)_5$, $CpMn(CO)_3$, $Os_3(CO)_{12}$, etc. We have reported[1c] that this approach is successful in conferring unusually high reactivity on $Cp^*Ru(PR_3)(OR_f)$.

In trying to generalize our ideas to a broader range of potential π-donor ligands X, we felt the need to develop a scale of comparative X-ligand ($\sigma + \pi$) donor power. To that end, it seemed desirable to incorporate into a molecule $MXL'L_n$ a reporter ligand L′, which would permit evaluation of relative X-ligand donor power. The CO stretching frequency has traditionally been used for this purpose in other contexts, and we therefore set out to synthesize a series of compounds embracing the widest possible range of groups X. Given the existence of species $MHCl(CO)P_2$ (M = Ru, Os; P = phosphine), whose reactivity was already proven[2] to be facile and versatile, we chose this as the reagent class from which to synthesize our series. Since ruthenium compounds generally display greater reactivity than osmium compounds, we chose this lighter metal for our study. We report here the most comprehensive evaluation to date of X-ligand donor power. With the experimental trend of comparative donor power established, it is necessary to understand the factors which control ν(CO). Only with such understanding can rational control of chemical reactivity be achieved. The effectiveness of such X-ligand optimization of reactivity is exemplified by studies of the influence of the fluoroalkoxide ligand on olefin metathesis catalysis.[3] We therefore report *ab initio* calculations of the CO stretching frequencies. No comparably extensive set of CO frequency calculations has ever been attempted. We place special emphasis on understanding the (surprising) donor power of fluoride in comparison to that of the heavier halides. As the following report will show, the CO ligand is not merely the innocent "reporter" we initially envisioned, but instead plays an active role in the electronic structure of the species $RuHX(CO)P_2$.

† Indiana University.
‡ Permanent address: Laboratory for Applied Quantum Chemistry, Department of Chemistry, University of Thessaloniki, 54006 Thessaloniki, Greece.
§ Université de Paris-Sud.
⊗ Abstract published in *Advance ACS Abstracts*, March 1, 1994.
(1) (a) Goldman, A. S.; Halpern, J. *J. Organomet. Chem.* **1990**, *382*, 237. (b) Lunder, D. M.; Lobkovsky, E. B.; Streib, W. E.; Caulton, K. G. *J. Am. Chem. Soc.* **1991**, *113*, 1837. (c) Johnson, T. J.; Huffman, J. C.; Caulton, K. G. *J. Am. Chem. Soc.* **1992**, *114*, 2725.
(2) Werner, H.; Esteruelas, M. A.; Otto, H. *Organometallics* **1986**, *5*, 2295.
(3) Schrock, R. R. *Acc. Chem. Res.* **1989**, *19*, 342; **1990**, *23*, 158.

0020-1669/94/1333-1476$04.50/0

Experimental Section

General Data. All manipulations were carried out using standard Schlenk and glovebox techniques under prepurified argon. Bulk solvents (toluene, hexanes [bp 68.6–69.3 °C]) were dried and deoxygenated over sodium or potassium benzophenone ketyl and subjected to three freeze–pump–thaw cycles prior to use. Deuterated solvents (C_6D_6, C_7D_8) were dried over sodium metal and vacuum distilled prior to use. NaBr, NaI, CsF, KOH, and $KOSiMe_3$ were purchased from Aldrich and used without further purification. Reagents KOEt, $KOCH_2CF_3$, $KOSiMe_2Ph$, $KOSiPh_3$, $KOCPh_3$, and KOPh were prepared by reacting the parent alcohol with KH. Reagent NaSPh was prepared by reacting PhSH with Na metal. Reagents LiC_2Ph and LiNHPh were prepared from PhC_2H and $PhNH_2$ and ^nBuLi, respectively. Carbon monoxide (99.9%) from Air Products Corp. was used without further purification. ^1H (referenced via residual solvent impurity), ^2H, ^{31}P (referenced to 85% H_3PO_4), and ^{19}F (referenced via CF_3CO_2H as −78.45 ppm) NMR spectra were recorded on a Nicolet NT-360 spectrometer operating at 360, 55, 146, and 331 MHz, respectively. ^{13}C NMR spectra were recorded on a Bruker AM-500 spectrometer at 125 MHz. Infrared spectra were recorded in C_6D_6 (NaCl cavity cell, 0.1 mm path length) on a Nicolet 510P FT-IR spectrometer to a precision of 0.3 cm^{-1}. Purity of those compounds prepared only for IR spectroscopic investigation was established by ^1H and $^{31}P\{^1H\}$ NMR and by IR (1600–2300 cm^{-1}).

$RuHI(CO)(P^tBu_2Me)_2$. To a toluene solution of 0.20 g (0.4 mmol) of $RuHCl(CO)(P^tBu_2Me)_2$[4] was added 0.5 g (3.4 mmol) of NaI. The slurry was stirred for 12 h and filtered through a medium-porosity frit. The solvent was removed under vacuum, and the resulting orange solid washed once with 2 mL of cold hexanes. Yield: 0.21 g, 90%. ^1H NMR (C_6D_6, 25 °C): δ 1.75 (vt, 6H, PMe), 1.20 (vt, 18H, P^tBu), 1.19 (vt, 18H, P^tBu), −23.7 (t, J_{PH} = 20 Hz, 1H, Ru–H). $^{31}P\{^1H\}$ NMR (C_6D_6, 25 °C): δ 48.0 (s). IR: ν_{CO} = 1908 cm^{-1}.

$RuHF(CO)(P^tBu_2Me)_2$. To a toluene solution of 0.20 g (0.4 mmol) of $RuHCl(CO)(P^tBu_2Me)_2$ was added 0.4 g (2.6 mmol) of CsF. The slurry was stirred for 12 h and filtered through a medium-porosity frit. The solvent was removed under vacuum, and the resulting yellow-orange solid was washed with 2 mL of cold hexanes and dried under vacuum. Yield: 0.16 g, 83%. ^1H NMR (C_6D_6, 25 °C): δ 1.26 (vt, 18H, P^tBu), 1.21 (vt, 18H, P^tBu), 1.23 (vt, 6H, PMe), −24.0 (t of d, J_{HP} = 19 Hz, J_{HF} = 3 Hz, 1H, Ru–H). $^{13}C\{^1H\}$ NMR (C_6D_6, 25 °C): δ 206.4 (dt, J_{CP} = 12 Hz, J_{CF} = 71 Hz, CO), 34.8 (vt, $PCMe_3$), 34.4 (vt, $PCMe_3$), 29.4 (br PCH_3, $PC(CH_3)_3$). $^{31}P\{^1H\}$ NMR (C_6D_6, 25 °C): δ 52.2 (d, J_{PF} = 24 Hz, 2P). ^{19}F NMR (C_6D_6, 25 °C): δ −311 (t, J_{FP} = 24 Hz, 1F). IR: ν_{CO} = 1892 cm^{-1}. Anal. Calcd for $RuOFP_2C_{19}H_{43}$: C, 48.60, H, 9.23. Found: C, 48.95; H, 9.55.

$RuHBr(CO)(P^tBu_2Me)_2$. To a solution of 0.02 g (0.04 mmol) of $RuHCl(CO)(P^tBu_2Me)_2$ in 0.5 mL of C_6D_6 was added 0.1 g (0.1 mmol) of NaBr. The resulting slurry was stirred for 12 h and filtered. Yield: 90%. ^1H NMR (C_6D_6, 25 °C): δ 1.54 (vt, 6H, PMe), 1.21 (vt, 18H, P^tBu), 1.19 (vt, 18H, P^tBu), −24.5 (t, J_{HP} = 20 Hz, 1H, Ru–H). $^{31}P\{^1H\}$ NMR (C_6D_6, 25 °C): δ 48.4 (s). IR: ν_{CO} = 1906 cm^{-1}.

$RuH(OCH_2CF_3)(CO)(P^tBu_2Me)_2$. To a solution of 0.02 g (0.04 mmol) of $RuHCl(CO)(P^tBu_2Me)_2$ in 0.5 mL of C_6D_6 was added 0.06 g (0.04 mmol) of $KOCH_2CF_3$. The resulting solution was stirred for 10 min and filtered. Yield: 99%. ^1H NMR (C_6D_6, 25 °C): δ 4.37 (q, J_{HF} = 7 Hz, 2H, OCH_2CF_3), 1.21 (vt, 6H, PMe), 1.13 (vt, 18H, P^tBu), 1.11 (vt, 18H, P^tBu), −25.0 (t, J_{HP} = 20 Hz, 1H, Ru–H). $^{31}P\{^1H\}$ NMR (C_6D_6, 25 °C): δ 56.3 (s). IR: ν_{CO} = 1892 cm^{-1}.

$RuH(OPh)(CO)(P^tBu_2Me)_2$. To a solution of 0.02 g (0.04 mmol) of $RuHCl(CO)(P^tBu_2Me)_2$ in 0.5 mL of C_6D_6 was added 0.005 g (0.04 mmol) of KOPh. The solution was stirred for 20 min and filtered. Yield: 85%. ^1H NMR (C_6D_6, 25 °C): δ 7.34 (t, J = 8 Hz, 2H, OPh), 6.74 (m, 3H, OPh), 1.13 (vt, 18H, P^tBu), 1.12 (vt, 18H, P^tBu), 1.02 (vt, 6H, PMe), −24.7 (t, J_{HP} = 19 Hz, 1H, Ru–H). $^{31}P\{^1H\}$ NMR (C_6D_6, 25 °C): δ 59.6 (s). IR: ν_{CO} = 1898 cm^{-1}.

$RuH(SPh)(CO)(P^tBu_2Me)_2$. To a solution of 0.02 g (0.04 mmol) of $RuHCl(CO)(P^tBu_2Me)_2$ in 0.5 mL of C_6D_6 was added 0.007 g (0.04 mmol) of NaSPh. The solution was stirred for 20 min and filtered. Yield: 70%. ^1H NMR (C_6D_6, 25 °C): δ 7.17 (m, 2H, SPh) 7.01 (m, 2H, SPh), 6.89 (m, 1H, SPh), 1.36 (vt, 6H, PMe), 1.18 (vt, 18H, P^tBu), 1.17 (vt, 18H, P^tBu), −23.9 (t, J_{HP} = 19 Hz, 1H, Ru–H). $^{31}P\{^1H\}$ NMR (C_6D_6, 25 °C): δ 52.0 (s). IR: ν_{CO} = 1904 cm^{-1}.

$RuH(OH)(CO)(P^tBu_2Me)_2$. To a solution of 0.02 g (0.04 mmol) of $RuHCl(CO)(P^tBu_2Me)_2$ in 0.5 mL of C_6D_6 was added 0.01 g (0.08 mmol) of KOH. The slurry was stirred for 2 h and filtered. Yield: 73%. ^1H NMR (C_6D_6, 25 °C): δ 2.55 (br, 1H, OH), 1.24 (vt, 18H, P^tBu), 1.24 (vt, 6H, PMe), 1.22 (vt, 18H, P^tBu), −22.3 (t, J_{HP} = 19 Hz, 1H, Ru–H). $^{31}P\{^1H\}$ NMR (C_6D_6, 25 °C): δ 57.6 (s). IR: ν_{OH} = 3667, ν_{CO} = 1896 cm^{-1}.

$RuH(OSiPh_3)(CO)(P^tBu_2Me)_2$. To a solution of 0.02 g (0.04 mmol) of $RuHCl(CO)(P^tBu_2Me)_2$ in 0.5 mL of C_6D_6 was added 0.013 g (0.04 mmol) of $KOSiPh_3$. The solution was stirred for 10 min and filtered. Yield: 90%. ^1H NMR (C_6D_6, 25 °C): δ 8.00 (br, 6H, $OSiPh_3$), 7.27 (br, 9H, $OSiPh_3$), 1.15 (vt, 18H, P^tBu), 1.12 (vt, 18H, P^tBu), 0.681 (vt, 6H, PMe), −24.9 (t, J_{HP} = 20 Hz, 1H, Ru–H). $^{31}P\{^1H\}$ NMR (C_6D_6, 25 °C): δ 58.6 (s). IR: ν_{CO} = 1890 cm^{-1}. Anal. Calcd for $RuSiP_2O_2C_{37}H_{58}\cdot C_6D_6$: C, 63.75; H, 7.22. Found: C, 63.21; H, 7.08.

$RuH(OSiMe_2Ph)(CO)(P^tBu_2Me)_2$. To a solution of 0.02 g (0.04 mmol) of $RuHCl(CO)(P^tBu_2Me)_2$ in 0.5 mL of C_6D_6 was added 0.008 g (0.04 mmol) of $KOSiMe_2Ph$. The solution was stirred for 10 min and filtered. Yield: 88%. ^1H NMR (C_6D_6, 25 °C): δ 7.98 (t, 2H, OSiPh), 7.40 (t, 2H, OSiPh), 7.28 (t, 1H, OSiPh), 1.18 (vt, 18H, P^tBu), 1.14 (vt, 18H, P^tBu), 1.06 (vt, 6H, PMe), 0.58 (br, 6H, OSiMe), −23.7 (t, J_{HP} = 19 Hz, 1H, Ru–H). $^{31}P\{^1H\}$ NMR (C_6D_6, 25 °C): δ 56.3 (s). IR: ν_{CO} = 1888 cm^{-1}.

$RuH(OSiMe_3)(CO)(P^tBu_2Me)_2$. To a solution of 0.02 g (0.04 mmol) of $RuHCl(CO)(P^tBu_2Me)_2$ in 0.5 mL of C_6D_6 was added 0.008 g (0.06 mmol) of $KOSiMe_3$. The solution was stirred for 10 min and filtered. Yield: 82%. ^1H NMR (C_6D_6, 25 °C): δ 1.24 (vt, 6H, PMe), 1.21 (vt, 18H, P^tBu), 1.16 (vt, 18H, P^tBu), 0.284 (s, 9H, $OSiMe_3$), −23.4 (t, J_{HP} = 19 Hz, 1H, Ru–H). $^{31}P\{^1H\}$ NMR (C_6D_6, 25 °C): δ 54.5 (s). IR: ν_{CO} = 1886 cm^{-1}.

$RuH(OCPh_3)(CO)(P^tBu_2Me)_2$. To a solution of 0.03 g (0.06 mmol) of $RuHCl(CO)(P^tBu_2Me)_2$ in 0.5 mL of C_6D_6 was added 0.018 g (0.06 mmol) of $KOCPh_3$. The solution was stirred for 30 min, after which $^{31}P\{^1H\}$ NMR shows 90% conversion to $RuH(OCPh_3)(CO)(P^tBu_2Me)_2$. ^1H NMR (C_6D_6, 25 °C): 7.34 (d, J = 6 Hz, 6H, *ortho*), 7.06 (m, 6H, *meta*), 7.05 (t, J = 6 Hz, 3H, *para*), 1.21 (vt, 18H, P^tBu), 1.18 (vt, 18H, P^tBu), 1.16 (vt, 6H, PMe), −22.7 (t, J_{PH} = 18 Hz, Ru–H). $^{31}P\{^1H\}$ NMR (C_6D_6, 25 °C): δ 53.1 (s). IR: ν_{CO} = 1885 cm^{-1}.

$RuH[OB(Mes)_2](CO)(P^tBu_2Me)_2$. To a solution of 0.02 g (0.04 mmol) of $RuHCl(CO)(P^tBu_2Me)$ in 0.5 mL of C_6D_6 was added 0.012 g (0.04 mmol) $[(LiOB(Mes)_2)(OEt_2)]_2$.[5] The solution was stirred for 2 days after which time, $^{31}P\{^1H\}$ NMR shows 75% conversion to $RuH[OB(Mes)_2](CO)(P^tBu_2Me)_2$. ^1H NMR (C_6D_6, 25%): δ 6.71 (s, 4H, *meta* H), 2.47 (s, 6H, *para* CH_3), 2.31 (s, 12H, *ortho* CH_3), 1.13 (vt, 18H, P^tBu), 1.07 (vt, 18H, P^tBu), 1.00 (vt, 6H, PMe), −24.0 (t, J_{PH} = 19 Hz, Ru–H). $^{31}P\{^1H\}$ NMR (C_6D_6, 25 °C): δ 55.8. $^{11}B\{^1H\}$ NMR (C_6D_6, 25 °C): δ 48.2 IR: ν_{CO} = 1896 cm^{-1}.

$RuH(C{\equiv}CPh)(CO)(P^tBu_2Me)_2$. To a solution of 0.02 g (0.04 mmol) of $RuHCl(CO)(P^tBu_2Me)_2$ in 0.5 mL of C_6D_6 was added 0.005 g (0.05 mmol) of LiC_2Ph. The solution was stirred for 12 h and filtered. Yield: 86%. ^1H NMR (C_6D_6, 25 °C): δ 7.60 (d, J = 7 Hz, 2H, Ph), 7.18 (t, J = 7 Hz, 2H, Ph), 7.01 (t, J = 7 Hz, 1H, Ph), 1.64 (vt, 6H, PMe), 1.21 (vt, 18H, P^tBu), 1.19 (vt, 18H, P^tBu), −27.9 (t, J = 19 Hz, 1H, Ru–H). $^{31}P\{^1H\}$ NMR (C_6D_6, 25 °C): δ 53.2 (s). $^{13}C\{^1H\}$ NMR (90 MHz, C_6D_6, 25 °C) of $RuH(^{13}CCPh)(CO)(P^tBu_2Me)_2$: δ 140.7 (t, J_{PC} = 20 Hz). IR: ν_{CO} = 1906 cm^{-1}, ν_{CC} = 2072 cm^{-1}.

$RuH(NHPh)(CO)(P^tBu_2Me)_2$. To a solution of 0.02 g (0.04 mmol) of $RuHCl(CO)(P^tBu_2Me)_2$ in 0.5 mL of C_6D_6 was added 0.005 g (0.04 mmol) of LiNHPh. The solution was stirred for 10 min and filtered. Yield: 65%. ^1H NMR (C_6D_6, 25 °C): δ 7.19 (t, 2H, NPh), 6.48 (t, 1H, NPh), 6.02 (br, 2H, NPh), 1.11 (vt, 36H, P^tBu), 1.13 (vt, 6H, PMe), −26.2 (t, J_{HP} = 20 Hz, 1H, Ru–H). No signal assignable to N–H was observed at +25 or −85 °C (C_7D_8). $^{31}P\{^1H\}$ NMR (C_6D_6, 25 °C): δ 57.6 (s). IR: ν_{CO} = 1898 cm^{-1}.

$RuHCl(CO)(P^tBu_2Me)_2 + PMe_3$. To a solution of 0.025 g (0.05 mmol) of $RuHCl(CO)(P^tBu_2Me)_2$ in 0.5 mL of C_6D_6 was added 3 μL (0.03 mmol) of PMe_3. ^1H and $^{31}P\{^1H\}$ NMR reveals (after 10 min at 25 °C) the production of $RuHCl(CO)(P^tBu_2Me)_2(PMe_3)$ and $RuHCl(CO)(P^tBu_2Me)(PMe_3)_2$ in a 1:3 ratio. $RuHCl(CO)(P^tBu_2Me)_2(PMe_3)$; $^{31}P\{^1H\}$ NMR (C_6D_6, 25 °C): δ 57.6 (d, J_{PP} = 18 Hz, 2P, P^tBu_2Me), −9.8 (t, J_{PP} = 18 Hz, 1P, PMe_3). Selected ^1H NMR (C_6D_6, 25 °C): δ −6.90 (d of t, $J_{HP^tBu_2Me}$ = 24 Hz, J_{HPMe_3} = 122 Hz, Ru–H). $RuHCl(CO)(P^tBu_2Me)(PMe_3)_2$; $^{31}P\{^1H\}$ NMR (C_6D_6, 25 °C): δ 57.2 (d of d, J = 20 Hz, J = 280 Hz, 1P, P^tBu_2Me), −1.1 (d of d, J = 19 Hz, J = 280 Hz, 1P, PMe_3), −23.7 (d of d, J = 19 Hz, J = 20 Hz, 1P, PMe_3). Selected

(4) Poulton, J. T.; Folting, K.; Streib, W. E.; Caulton, K. G. *Inorg. Chem.* **1992**, *31*, 3190. $^{31}P\{^1H\}$ NMR (−85 °C, toluene-d_8): δ 55.6, 53.9 (AB line unresolved from the M_2 line), 41.9, 40.1 ppm (J_{AB} = 265 Hz).

(5) Weese, K. J.; Bartlett, R. A.; Murray, B. D.; Olmstead, M. M.; Power, P. P. *Inorg. Chem.* **1987**, *26*, 2649.

Table 1. CO Stretching Frequencies (cm^{-1})

X	$RuHX(CO)(P^tBu_2Me)_2$	$RuHX(CO)(py)(P^tBu_2Me)_2$
H	*a*	1902
I	1908	1889
Br	1906	1885
C≡CPh	1906	*a*
Cl	1904	1884
SPh	1904	*a*
OPh	1898	1879
NHPh	1898	1885
OH	1896	1883
$OB(Mesityl)_2$	1896	1876
OCH_2CF_3	1892	1873
F	1892	1869
$OSiPh_3$	1890	1875
$OSiMe_2Ph$	1888	1871
$OSiMe_3$	1886	1871
$OCPh_3$	1885	1869
OEt	1883	1867

[a] Not available.

^1H NMR (C_6D_6, 25 °C): δ −7.0 (d of d of d, J = 24 Hz, J = 28 Hz, J = 122 Hz, 1H, Ru–H).

$RuH(OCH_2CH_3)CO(P^tBu_2Me)_2$. To a solution of 0.04 g (0.08 mmol) of $RuHCl(CO)(P^tBu_2Me)_2$ in 0.5 mL of C_6D_6 was added 0.007 g (0.08 mmol) of KOC_2H_5. The resulting solution was quickly filtered. ^1H NMR (C_6D_6, 25 °C): 4.08 (br, 2H, OCH_2CH_3), 1.39 (br, 9H, overlapping PMe and OCH_2CH_3), 1.23 (vt, 18H, P^tBu), 1.20 (vt, 18H, P^tBu), −24.2 (t, J_{HP} = 19 Hz, 1H, Ru–H). $^{31}P\{^1H\}$ NMR (C_6D_6, 25 °C): 55.5 (s). IR: ν_{CO} = 1883 cm^{-1}. In solution, this compound decomposes ($t_{1/2} \approx$ 30 min) to several products as assayed by ^{31}P NMR.

Pyridine Adducts of $RuHX(CO)(P^tBu_2Me)_2$. All $RuHX(CO)(P^tBu_2Me)_2$ species bind pyridine (py) reversibly, unlike the PMe_3 case. Excess pyridine (~5 equiv) is required to obtain NMR data for the fully formed (>95%) adduct at 25 °C. Spectra collected at 25 °C show by both ^1H and $^{31}P\{^1H\}$ NMR one set of resonances in the presence of 0.5 or 5 equiv of py. The most diagnostic NMR change occurring upon addition of py is a downfield shift of the ^1H NMR hydride signal (by 10–12 ppm). For X = $OSiPh_3$, I, and OCH_2CF_3, at high py:Ru ratios (~4 equiv) traces of a bis(pyridine) adduct *cis*-$RuHX(CO)(P^tBu_2Me)(py)_2$ may be observed as identified by a ^1H NMR hydride doublet and concomitant production of free P^tBu_2Me observed at 11.7 ppm by $^{31}P\{^1H\}$ NMR. ^1H and $^{31}P\{^1H\}$ parameters for $RuH(OCH_2CF_3)(CO)(P^tBu_2Me)_2(py)$ were recorded at −60 °C at which temperature pyridine dissociation and rotation around the Ru–N bond is slow on the (360-MHz) NMR time scale. NMR data for $RuH(OCH_2CF_3)(CO)(P^tBu_2Me)_2(py)$ as follows. ^1H NMR (C_7D_8, −60 °C): δ 9.71 (d, J = 5 Hz, 1H, py), 8.70 (d, J = 5 Hz, 1H, py), 6.69 (m, 1H, py), 6.52 (m, 1H, py), 6.27 (m, 1H, py), 4.27 (br, 2H, OCH_2CF_3), 1.22 (br, 6H, PMe), 1.09 (br, 36H, P^tBu), −13.3 (t, J_{HP} = 22 Hz, 1H, Ru–H). $^{31}P\{^1H\}$ NMR (C_7D_8, −60 °C): δ 46.7 (br, 2P). $^{31}P\{^1H\}$ NMR (C_7D_8, −85 °C): δ 55.2 (d, J_{PP} = 306 Hz, 1P), 38.4 (d, J_{PP} = 306 Hz, 1P). Additional evidence for the equilibrium nature of these reactions is obtained from infrared spectroscopy (a faster spectroscopic technique) which clearly shows a CO stretching band for $RuH(OCH_2CF_3)(CO)(P^tBu_2Me)_2$ and for $RuH(OCH_2CF_3)(CO)(P^tBu_2Me)_2(py)$ in the presence of 0.5 equiv of pyridine. Table 1 contains ν_{CO} data for selected $RuHX(CO)(P^tBu_2Me)_2(py)$ species.

$RuHF(CO)_2(P^tBu_2Me)_2$. A C_6D_6 solution of 0.02 g of $RuHF(CO)(P^tBu_2Me)_2$ (0.04 mmol) was placed in an NMR tube fitted with a teflon stopcock. The solution was frozen in liquid N_2, the headspace evacuated, and 1 atm of CO (0.1 mmol) introduced into the tube. Upon thawing, the initially light-orange solution became lemon yellow. Yield: 97%. ^1H NMR (C_6D_6, 25 °C): δ 1.41 (vt, 6H, PMe), 1.32 (vt, 18H, P^tBu), 1.22 (vt, 18H, P^tBu), −4.16 (d of t, J_{PH} = 19 Hz, J_{PH} = 9 Hz, 1H, Ru–H). $^{31}P\{^1H\}$ NMR (C_6D_6, 25 °C): δ 63.9 (d, J_{PF} = 20 Hz). ^{19}F NMR (C_6D_6, 25 °C): δ −202 (t, J_{PF} = 20 Hz). $^{13}C\{^1H\}$ NMR (C_6D_6, 25 °C): δ 204.6 (d of t, $J_{CF_{trans}}$ = 67 Hz, J_{CP} = 12 Hz, CO), 199.0 (d of t, $J_{CF_{cis}}$ = 9 Hz, J_{CP} = 6 Hz, CO), 35.3 (vt, P–CMe_3), 35.2 (vt, PCMe_3), 29.7 (s, overlapping signals for P–CH_3 and P–C(CH_3)$_3$), 29.3 (s, P–C(CH_3)$_3$). IR: ν_{CO} = 2029, 1912 cm^{-1}.

Structure Determination of $RuH(OSiPh_3)(CO)(P^tBu_2Me)_2$. A suitable single crystal was selected from the bulk sample using inert-atmosphere handling techniques. The crystal was affixed to a glass fiber with silicone grease and was transferred to the goniostat, where it was cooled to −160 °C for characterization (Table 2) and data collection (6° < 2θ < 45°). A systematic search of a limited hemisphere of reciprocal space yielded a set of reflections which exhibited monoclinic ($2/m$) symmetry. The systematic extinction of $h0l$ for $h + l = 2n + 1$ and of $0k0$ for $k = 2n + 1$ uniquely identified the space group as $P2_1/n$ (No. 14). This choice was confirmed by the subsequent solution and refinement of the structure. Four standard reflections monitored every 100 reflections showed no systematic trends. No correction for absorption was carried out. The structure was solved by locating the Ru and P atoms using SHELXS-86. The remainder of the non-hydrogen atoms were located in successive cycles of difference Fourier iterations. The asymmetric unit was found to contain two independent molecules ("A" and "B") as well as a half-molecule of benzene solvent. The solvent carbon atoms are numbered C(87) to C(89). Following initial refinement about half of the hydrogen atoms were evident in a difference map. The full-matrix least-squares refinement was completed using anisotropic thermal parameters on all non-hydrogen atoms. The hydrogen atoms were introduced in fixed calculated positions, having a B value of 1 $Å^2$ plus the isotropic equivalent of the parent atom. The final difference map was essentially featureless, the largest peak being 1.04 $e/Å^3$. Several peaks were located in the immediate vicinity (within 1.3 Å) of the Ru atoms, however, none could be interpreted as hydride positions. The results of the structure determination are shown in Figure 1 and Table 3.

Table 2. Crystallographic Data[a] for $RuH(OSiPh_3)CO(P^tBu_2Me)_2$

formula	$C_{37}H_{58}O_2P_2RuSi \cdot {}^1/_2C_6H_6$	fw	1530.05
a, Å	11.263(1)	space group	$P2_1/n$
b, Å	31.713(4)	T, °C	−160 °C
c, Å	22.311(3)	λ, Å	.71069
β, deg	100.07(0)	ρ_{calcd}, g cm^{-3}	1.295
V, $Å^3$	7846.65	R	.0541
Z	4	R_w	.0545

[a] $R = \Sigma||F_o| - |F_c||/\Sigma|F_o|$. $R_w = [\Sigma w(|F_o| - |F_c|)^2/\Sigma w/F_o|^2]^{1/2}$, where $w = 1/\sigma^2(|F_o|)$.

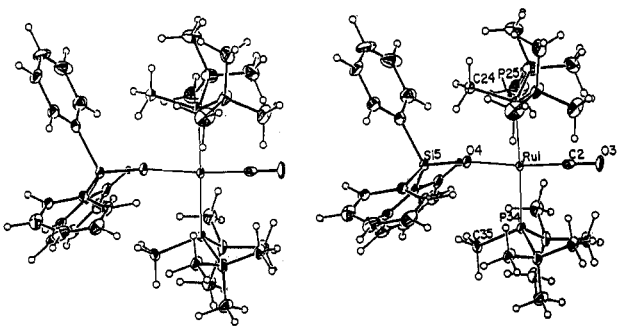

Figure 1. Stereo ORTEP drawing of the nonhydrogen atoms of one independent molecule of $RuH(OSiPh_3)(CO)(P^tBu_2Me)_2$, showing selected atom labeling.

Table 3. Selected Bond Distances (Å) and Angles (deg) for $RuH(OSiPh_3)(CO)(P^tBu_2Me)_2$

	molecule A	molecule B
Ru(1)–P(24)	2.3737(18)	2.3788(17)
Ru(1)–P(34)	2.3890(17)	2.3819(17)
Ru(1)–O(4)	2.057(4)	2.057(4)
Ru(1)–C(2)	1.819(6)	1.800(6)
P(24)–C(25)	1.815(6)	1.828(7)
P(24)–C(26)	1.875(7)	1.893(7)
P(24)–C(30)	1.879(7)	1.878(7)
P(34)–C(35)	1.820(6)	1.828(6)
P(34)–C(36)	1.889(7)	1.896(6)
P(34)–C(40)	1.889(6)	1.892(7)
Si(5)–O(4)	1.584(4)	1.588(4)
O(3)–C(2)	1.160(7)	1.172(7)
P(24)–Ru(1)–P(34)	175.00(6)	177.27(6)
P(24)–Ru(1)–O(4)	87.71(13)	88.91(12)
P(24)–Ru(1)–C(2)	91.61(19)	90.65(20)
P(34)–Ru(1)–O(4)	91.66(12)	91.95(12)
P(34)–Ru(1)–C(2)	90.36(19)	89.12(20)
O(4)–Ru(1)–C(2)	163.87(23)	166.42(25)
O(4)–Si(5)–C(6)	113.69(26)	112.97(25)
O(4)–Si(5)–C(12)	110.38(26)	111.68(26)
O(4)–Si(5)–C(18)	108.85(26)	109.78(25)
Ru(1)–O(4)–Si(5)	168.8(3)	162.21(28)
Ru(1)–C(2)–O(3)	177.4(6)	177.7(6)

Computational Details

(a) EHT PES for $RuH(CO)(OH)(PH_3)_2$. EHT calculations (with weighted H_{ij} formula) used atomic parameters from the literature.[6] Experimental phosphine ligands were replaced by PH_3 and the Ru–P bonds were kept perpendicular to the mirror plane containing Ru, H, OH, and CO. All distances were taken from the crystal structure of $RuH(CO)(OSiR_3)(PR_3)_2$ and were kept constant for the whole calculation of the potential energy surface (PES).

(b) Ab Initio Calculations. All calculations were carried out by an *ab initio* method at the Hartree–Fock (HF)–SCF level using the effective core potential (ECP) approximation for the inner core electrons of the Ru, Si, P and Cl atoms. For Ru, the ECP of Hay and Wadt, which includes the 4s and 4p electron in the valence shell, was chosen,[7] with a (6s6p5d) Gaussian basis set contracted into [3111/3111/311] for the valence shell. For Cl, Si, and P, we chose a (4s4p) Gaussian basis set contracted into [31/31], with the ECP's of Barthelat *et al.* for Cl[8] and of Stevens and Basch for Si and P.[9a] The basis set of Si was augmented with one set of d-polarized functions[7b] (ζ = 0.395). For H, the (5s) primitives of Huzinaga contracted into a [311] basis set was used for all H except those of PH_3, CH_3, and OH groups where (4s) primitives were contracted into [1s].[10] For C, O, and F, the (9s5p) primitives of Huzinaga were contracted into the split valence [721/41] of Dunning and Hay.[11]

Molecular geometries of all the complexes studied were fully optimized at the HF level using an analytical gradient under C_s constraint, with residual forces less than 5×10^{-4} hartree/bohr. We have learned from our previous study[12] of other d^6 ML_5 that the PES could be calculated with a single configuration in most of the space except in the region close to that of a trigonal bipyramidal structure, where there is a very small HOMO-LUMO gap (Jahn–Teller active system). Since we also know that this structure[12] is a high energy point and since we are interested in other parts of the space, we could represent the wave function by a single configuration. However, the metal–CO back-bonding interaction is poorly represented at the HF level. Therefore, the interatomic Ru–C and C–O distances were optimized (keeping the other structural parameters constant) with the second-order Møller–Plesset (MP2) perturbation calculations. All calculations were performed with the GAMESS package on a SUN SPARC MP 670 and on an IBM RISC 6000/530 workstation.[13]

Results

Synthesis and Spectroscopic Characterization of $RuHX(CO)P_2$ Compounds. With proper attention to the halide transfer reagent, the chloride in $RuHCl(CO)P_2$ can be transformed into numerous other halide compounds. Excess amounts of the salts NaI, NaBr, and CsF react within 12 h at 25 °C in benzene or hexane to give complete conversion. The salts KI, KBr, NaF, and AgF all fail to deliver product in good yield, illustrating the importance of counterion (and lattice energy) on these metathesis reactions.

The species $RuHX(CO)P_2$ with X = OCH_2CF_3, OPh, SPh, $OCPh_3$, $OSiMe_nPh_{3-n}$, and NHPh are conveniently synthesized from KX or NaX and $RuHCl(CO)P_2$ in benzene. Because these alkali metal reagents are more soluble, the metathesis reactions are complete within 30 min at 25 °C. Reaction with (insoluble) KOH requires 2 h.

Structure of $RuH(OSiPh_3)CO(P^tBu_2Me)_2$. The unit cell contains two crystallographically independent molecules of $RuH(OSiPh_3)CO(P^tBu_2Me)_2$. A best least-squares fit of the Ru(CO)(OSi) portions of the two molecules shows these atoms to deviate by at most 0.08 Å. The largest deviations occur between the phenyl rings, but even these adopt the same general conformation. A drawing of the two superimposed structures is included as supplementary material.

The structure (Figure 1) conforms closely to square-pyramidal geometry. The hydride hydrogen was not located, but is presumed to lie on one side of the $RuP_2(O)(C)$ plane. The bending of the basal groups away from the apical (hydride) ligand is very small in this molecule because of the increased repulsions which would result when the $OSiPh_3$ ligands approach both P^tBu_2Me ligands at angles less than 90°. This is also evident in the fact that all *four* phosphine ligands direct the smaller methyl substituent towards the $OSiPh_3$ group. It is also true that the P–CH_3 distances are systematically shorter than the P–CMe_3 distances.

The Ru–C–O angles are within 2.6° of linear while the Ru–O–Si distances deviate by 11.2 and 17.8° from linearity. The moderate bend which occurs at the siloxide oxygen is in the idealized molecular mirror plane, and the Si–O bond conformation directs two phenyl substituents toward the side of the square base trans to the hydride.

There is no evidence for agostic Ru/H interactions. The shortest Ru/H distances (all intramolecular) are 2.88 (molecule A) and 2.86 Å (molecule B), which are longer than the very weak contact (2.59 Å) in $RuCl_2(PPh_3)_3$.[14]

The Ru–CO distance (1.81 Å) is very short,[15] which is consistent with the presence of a push–pull interaction from $OSiPh_3$ lone pairs into the CO π^* orbitals. The Ru–P distances (2.37–2.39 Å) are comparable to those from Ru(II) to PEt_3, PPh_3, PMe_2Ph, and $PMePh_2$, but are distinctly shorter than those involving P^tBu_3 (2.52–2.62 Å). The Ru–O distance (2.057 Å) is shorter than that in $RuH(OC_6H_4$-*p*-$Me)(PMe_3)_4$ (2.145 Å)[16] which suggests the presence of an Ru/O multiple bond in $RuH(OSiPh_3)(CO)(P^tBu_2Me)_2$.

Evidence for Steric Influence. The steric crowding within these molecules introduced by the bulky P^tBu_2Me groups is manifest in their low-temperature $^{31}P\{^1H\}$ NMR spectra. The $^{31}P\{^1H\}$ NMR singlet observed for $RuHCl(CO)P_2$ at 25 °C in toluene collapses and then resolves into four lines by −85 °C. These can be analyzed[4] as an M_2 singlet and an AB pattern (there is one overlap of two lines) due to the

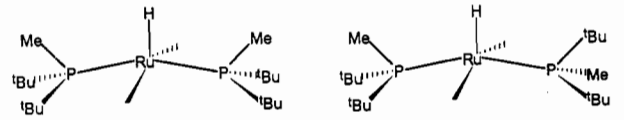

conformers having slow rates of interconversion. Rotation about the Ru–P bonds is now slow. This phenomenon has been extensively investigated by the group of Bushweller.[17] We note that $RuHI(CO)P_2$ shows $^{31}P\{^1H\}$ NMR broadening at −85 °C, but the spectral patterns of "frozen" conformers has not yet been resolved. This suggests that the P^tBu_2Me rotational barrier is lower for the iodide than for the chloride (cone angles[18] are I: 107°, Cl: 102°).

An Infrared Criterion of X Donor Power. The presence of a CO ligand was envisioned as serving as a reporter of back-bonding, and thus of donor power of the fragment $RuHCOP_2$ as the group X is varied. The CO stretching frequencies (Table 1) establish

(6) The weighted H_{ij} formula was used: Ammeter, J. H.; Bürgi, H.-B.; Thibeault, J. C.; Hoffmann, R. *J. Am. Chem. Soc.* **1978**, *100*, 3686. Atomic parameters for Ru: Thorn, D. L.; Hoffmann, R. *Inorg. Chem.* **1976**, *17*, 126. Atomic parameters for P: Summerville, R. H.; Hoffmann, R. *J. Am. Chem. Soc.* **1970**, *98*, 7240.
(7) Hay, P. J.; Wadt, W. R. *J. Chem. Phys.* **1985**, *82*, 299.
(8) Bouteiller, Y.; Mijoule, C.; Nizam, N.; Barthelat, J.-C.; Daudey, J.-P.; Pélissier, M.; Silvi, B. *Mol. Phys.* **1988**, *65*, 295.
(9) (a) Stevens, W. J.; Basch, H.; Krauss, M. *J. Chem. Phys.* **1984**, *81*, 6026. (b) Gordon, M. S. *Chem. Phys. Lett.* **1980**, *76*, 163.
(10) Huzinaga, S. *J. Chem. Phys.* **1965**, *42*, 1293.
(11) Dunning, T. H.; Hay, P. J. In *Methods of Electronic Structure Theory*; Schaefer, H. F., III, Ed., Plenum Press: New York, 1977; Vol. 1.
(12) Riehl, J.-F.; Jean, Y.; Eisenstein, O.; Pélissier, M. *Organometallics* **1992**, *11*, 729.
(13) Schmidt, M. W.; Baldridge, K. K.; Boatz, J. A.; Jensen, J. H.; Koseki, S.; Gordon, M. S.; Nguyen, K. A.; Winndus, T. L.; Elbert, S. T. GAMESS (General Atomic and Molecular Electronic Structure System). *QCPE Bull.* **1990**, *10*, 52.
(14) LaPlaca, S. J.; Ibers, J. A. *Inorg. Chem.* **1965**, *4*, 778.
(15) Orpen, A. G.; Brammer, L.; Allen, F. H.; Kennard, O.; Watson, D. G.; Taylor, R. *J. Chem. Soc., Dalton Trans.* **1989**, S1.
(16) Osakada, K.; Ohshiro, K.; Yamamoto, A. *Organometallics* **1991**, *10*, 404.
(17) Bushweller, C. H.; Rithner, C. D.; Butcher, D. J. *Inorg. Chem.* **1986**, *25*, 1610.
(18) Tolman, C. A. *Chem. Rev.* **1977**, *77*, 313.

the following ranking of total (i.e., $\sigma + \pi$) ligand donor power:

$$OEt > OCPh_3 > OSiMe_3 > OSiMe_2Ph > OSiPh_3 > F \simeq OCH_2CF_3 > OH \approx OB(Mesityl)_2 > NHPh \simeq OPh > SPh \simeq Cl > C_2Ph \simeq Br > I$$

These show that the oxygen-based ligands are stronger donors than the halides.[19] The nitrogen-based and the oxygen-based ligands are comparable. The siloxides are better donors than phenoxide or OCH_2CF_3 (which is comparable to F), and replacing phenyl by methyl groups on a siloxide incrementally increases donor power. Donor power is higher for $OCPh_3$ than for $OSiPh_3$.

The ligand $OB(Mes)_2$ (Mes = mesityl) has been evaluated recently[5] as an alkoxide which should be a weak donor due to O→B π donation. We have made $RuH[OB(Mes)_2](CO)P_2$ by reaction of the chlororuthenium compound and $LiOB(Mes)_2$ in benzene. The CO stretching frequency of this product shows the $OB(Mes)_2$ ligand to be a weaker donor than all siloxides, but better than phenoxide. Somewhat surprisingly, it is comparable to hydroxide.

There are two other important trends within the data. One is that thiophenoxide is a weaker donor than phenoxide. The second is the closely related, but more fully documented trend up to the group of halides. Donor power increases by small, regular (2 cm^{-1}) increments along the series I < Br < Cl, followed by a considerably larger jump (12 cm^{-1}) to fluoride. This trend up to the halide group and up the chalcogen group is clearly opposite that predicted based on electronegativity, yet it is the same as observed for $IrXCO(PPh_3)_2$[20] and $CpRe(PR_3)(NO)X$.[21] We feel that this has received no satisfactory explanation in the literature and return to this subject below.

Metathesis of the chloride of $RuHCl(CO)P_2$ with LiC_2Ph in benzene gave a compound of interest because it contains no conventional (i.e., lone pair bearing) π-donor ligand: $RuH(C_2Ph)(CO)P_2$. We envisioned this σ-hydrocarbyl compound as being closer to a truly unsaturated species. However, its CO stretching frequency (1906 cm^{-1}) is identical to that of the bromo compound.[22] We are therefore forced to conclude that this compound experiences a degree of X→M π-donation from the filled acetylide π orbitals to the metal, thereby diminishing the coordinative unsaturation and lowering ν_{CO}. Moreover, we will report independently[23] the reaction in eq 2. Since there is evidence

$$RuH(OR)(CO)P_2 + PhC_2H \rightarrow RuH(C_2Ph)(CO)P_2 + ROH \quad (2)$$

for a strong Ru–O bond in the reactant complex, Ru/C_2Ph multiple bonding in the product complex is required if this reaction (eq 2) is to be exergonic. A similar conjugation has been reported recently in the case of a $W(CR)(C_2R)$ system.[24]

We originally envisioned that we could separate σ- and π-donor effects of the group X by recording the ν_{CO} values of the corresponding series of compounds $RuHX(CO)(L)P_2$ where L was a purely σ-donor ligand; we chose L = pyridine. Our reasoning was that, based on the 18-electron rule, addition of pyridine in a six-coordinate species $RuHX(CO)(L)P_2$ will use a metal d-orbital which will force the group X to bond in a purely σ fashion. That is, all lone pairs will become localized on X, and thus ν_{CO} in $RuHX(CO)(L)P_2$ will reflect the σ-donor power of X. The observed ν_{CO} values (Table 1) show precisely the same trend with X as do the values for the five-coordinate species. Moreover, the changes in ν_{CO} in the series are quite comparable in magnitude for the five- and the six-coordinate species. This could be used to conclude that either there is no π donation from X *or* that the coordination of pyridine does not disrupt π donation from X. We considered the latter option by a qualitative molecular orbital analysis,[4] which reveals that the π^* orbital of CO is of the proper symmetry to interact with the out-of-phase combination of the filled/filled d_π/X lone-pair couple and thereby relieves the four-electron destabilization. This means that the X→Ru π interaction is not eliminated in $RuHX(CO)(py)P_2$ species precisely because of the presence of our intended spectroscopic "reporter" ligand. The π-acid character of CO thus negates our supposition that a six-coordinate species will have a purely σ Ru–X bond, yet a compound without the CO ligand (e.g., $RuHX(py)_2P_2$) will have a purely σ Ru–X bond but has no reliable spectroscopic probe of metal electron density. This also indicates that the Ru–X bond length in any CO-containing six-coordinate d^6 Ru species is not a reliable indication of a single bond but retains some degree of multiple bond character; the X group is not simply a one-electron donor (neutral X formalism) in such a molecule. The experimental separation of σ- from π-donor effects of X ligands remains elusive.[25]

Evaluation of Hydride Donor Power. We will report separately the preparation of $Ru(H)_2(py)(CO)(P^tBu_2Me)_2$. The compound allows comparison of the donor power of a purely σ-donating hydride to the lone-pair bearing X groups in the six-coordinate $RuH(X)(CO)(py)(P^tBu_2Me)_2$. The observed ν_{CO} of 1902 cm^{-1} for $Ru(H)_2(py)(CO)(P^tBu_2Me)_2$ is noticably higher than any other value recorded here (the highest is 1889 cm^{-1} reported for X = I), indicating that H^- is the weakest donor available. This poorer donor ability of H^- is also reflected in the fact that the five-coordinate X = H species $Ru(H)_2(CO)(P^tBu_2Me)_2$ is not an isolable compound: it is too Lewis acidic to achieve detectable concentration. It readily binds H_2.[26]

Supporting Evidence for Fluoride Donor Character. (a) ^{19}F Chemical Shifts. The compound $RuHF(CO)P_2$ is a relatively rare case of a hydrido fluoro complex,[27] and provides rich NMR spectra. Fluorine couples to phosphorus, to the hydride, and to CO. The ^{19}F chemical shift in this molecule also provides a probe for the change of metal electronic structure on adding a sixth ligand: $RuHF(CO)P_2$ *vs* $RuHF(L)(CO)P_2$. We have evaluated cases where L is a predominantly σ-donor (pyridine) and a π-acceptor (CO). While $RuHF(CO)P_2$ shows a ^{19}F resonance at −311 ppm, $RuHF(py)(CO)P_2$ appears at −491 ppm. The latter is near the upfield limit of values reported for coordinated fluorine. The six-coordinate CO adduct $RuHF(CO)_2P_2$ has a ^{19}F chemical shift of −202 ppm, which is in the opposite direction to that found on coordinating pyridine. We propose that both of these effects are related to the extent of F→Ru π-donation. Coordination of pyridine decreases such π-donation by making the metal less electrophilic. Coordination of CO uses one metal σ orbital (as does pyridine), but it creates additional push–pull interactions wherein fluorine lone pairs, filled d_π orbitals, and empty CO π^* orbitals interact to enhance fluorine π-donation. There are two such interactions in $RuHF(CO)P_2$, but a third one is added in the dicarbonyl compound (**1**). It is noteworthy that the $^2J_{HRuF}$ value is dependent on the L in $RuHF(L)(CO)P_2$, having values of 2, 9, and 3 Hz when L is py, CO or absent, respectively.

(b) Hydrogen Bonding to Fluoride. The sensitivity of $\delta(^{19}F)$ to metal coordination number can be used to understand the interaction of $RuHF(CO)P_2$ with methanol in toluene. Addition

(19) It is significant that the labilizing power of the group X in $Co^{III}(H_2O)_5X^{2+}$ compounds via an S_N1CB mechanism is $NH_2 > OH > Cl$ (i.e., similar to the trend we report for ν_{CO}). See Tobe, M. L. *Acc. Chem. Res.* **1970**, *3*, 377.

(20) Vaska, L.; Peone, J. *Chem. Commun.* **1971**, 418.

(21) Merrifield, J. A.; Fernandez, J. M.; Buhro, W. E.; Gladysz, J. A. *Inorg. Chem.* **1984**, *23*, 4022.

(22) Since $RuH(^{13}CCPh)(CO)P_2$ has ν_{CO} only 2 cm^{-1} lower than the ^{12}C isotopomer, there is negligible mixing of ν_{CO} with $\nu_{C\equiv C}$.

(23) Poulton, J. T.; Sigalas, M.; Caulton, K. G. Eisenstein, O., *Inorg. Chem.* **1993**, *32*, 5490.

(24) Hanna, J.; Geib, S. J.; Hopkins, M. D. *J. Am. Chem. Soc.* **1992**, *114*, 9199.

(25) The hydride chemical shift of a pyridine adduct lies typically 8 ppm downfield of the five-coordinate analog.

(26) Gusev, D. G.; Vymenits, A. B.; Bakhmutov, V. I. *Inorg. Chem.* **1992**, *31*, 1.

(27) Doherty, N. M.; Hoffman, N. W. *Chem. Rev.* **1991**, *91*, 553. Massa, W.; Babel, D. *Chem. Rev.* **1988**, *88*, 275.

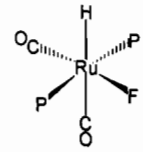

1

of 0.3 eq. MeOH to a toluene-d_8 solution of the fluoro compound causes a slight change in the ^1H NMR chemical shift of the hydride (from −24.02 to −24.08). The more sensitive ^{19}F chemical shift moves from −311 to −314 and more clearly establishes the occurrence of some interaction between $RuHF(CO)P_2$ and MeOH. This interaction could be hydrogen bonding to F and/or coordination of O to the Lewis acidic Ru. Given the magnitude (~7 ppm) of the change in hydride chemical shift upon addition of py to the $RuHX(CO)P_2$ species, the small change in hydride chemical shift induced by MeOH is not consistent with a change to a six-coordinate metal center. Coordination of methanol oxygen is also inconsistent with the new ν_{CO} observed in the presence of 0.3 equiv of MeOH (1902 cm^{-1}; the 1892 cm^{-1} species is also observed) compared to 1892 cm^{-1} for $RuHF(CO)P_2$ itself, which indicates that the metal has become *less* electron-rich. Six-coordinate species in this series have lower ν_{CO} values. Consequently, we conclude that hydrogen bonding causes the spectral changes that occur upon addition of 0.3 equiv of MeOH to $RuHF(CO)P_2$. Cooling this solution causes upfield movement of the ^{19}F chemical shift (−316 ppm at −15 °C, −317 ppm at −60 °C) with concomitant broadening of the signal. At the limiting temperature of −85 °C, the ^{19}F signal has nearly broadened into the baseline; decoalescence into two peaks is near. The ^1H NMR spectrum of this solution at −85 °C also shows only one set of peaks, but these are broadened (as is the $^{31}P\{^1H\}$ NMR spectrum).

We have also looked at a solution containing excess methanol. At −85 °C, a toluene-d_8 sample of $RuHF(CO)P_2$ containing 1.2 equiv of MeOH shows a broad ^{19}F signal centered at −349 ppm. The observation of one set of MeOH signals at ^1H NMR for this solution again indicates that MeOH exchange is fast even at −85 °C. Addition of a large excess of MeOH (10 equiv, −85 °C) results in a ^{19}F signal substantially farther upfield at −449 ppm, indicating that an additional interaction is present. This interaction could involve H bonding of a second mole of MeOH.[28]

Overall, these data are consistent with the occurrence of the equilibrium in eq 3 as a process which does not lie completely to the right (eq 3) at a 1:1 mole ratio and which is rapid on the ^1H,

$$RuHF(CO)P_2 + MeOH \rightleftharpoons MeOH\cdots FRuH(CO)P_2 \quad (3)$$

^{19}F (and also ^{31}P) NMR time scales at all accessible temperatures. The *important general conclusion from this study is that even a good donor such as fluoride retains considerable nucelophilic character*. This has implications for the hydrogenolysis of such bonds (eq 4).[23,29]

$$Ru{-}X + H_2 \rightarrow Ru{-}H + HX \quad (4)$$

A Reactivity Test of X-Ligand Donor Power. Lewis Acidity of $RuHX(CO)P_2$ Compounds. To the extent that a ligand X is a π donor, this might act to suppress the Lewis acidity of a compound which might otherwise be termed unsaturated. We carried out a few exploratory reactions of these five-coordinate compounds to evaluate this hypothesis.

Reaction of $RuHCl(CO)P_2$ at 25 °C with less than equimolar amounts of PMe_3 occurs rapidly. One product is **2** (together with unreacted $RuHCl(CO)P_2$). Proof that PMe_3 has added beneath the base of the reagent square pyramid (i.e., trans to hydride) comes from the large (i.e., trans) $J(H{-}PMe_3)$ value of 122 Hz. The P^tBu_2Me phosphorus nuclei are observed to be equivalent in the product. A second product, **3**, involves overall replacement of one P^tBu_2Me in **2** by PMe_3. Compound **3** shows one large $J(H{-}PMe_3)$ value (and one small one) and an AMX

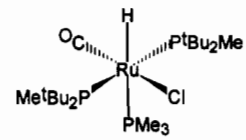

2

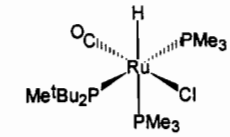

3

$^{31}P\{^1H\}$ NMR pattern. We suggest that **3** is mechanistically a product derived from **2** by reaction 5 and that this reaction occurs

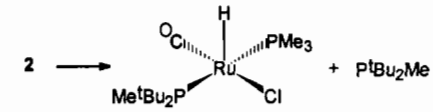

(5)

because of the crowded nature of **2** and the weaker binding of the bulky ligand P^tBu_2Me. The five-coordinate $RuHCl(CO)(P^tBu_2Me)(PMe_3)$ will be efficiently scavenged by available PMe_3 to generate **3**.

Analogous reactions are displayed by pyridine as nucleophile, with the distinction that the metal binding of pyridine is weaker than that of PMe_3. Thus, both the proton and phosphorus NMR spectra at 25 °C show continuous movement of chemical shifts as the mole ratio py:Ru increases from 0.5 to 5.0. This indicates that equilibrium 6 does not lie entirely to the right at a 1:1

$$RuH(OR_f)(CO)P_2 + py \rightleftharpoons RuH(OR_f)(CO)(py)P_2 \quad (6)$$

stoichiometry and that its rate is rapid on both NMR time scales. It was found that such exchange averaging can be halted at −60 °C for $RuH(OCH_2CF_3)(CO)(py)P_2$. At this temperature, there was ^{31}P NMR evidence (broad-line spectrum) for another dynamic process. At −85 °C, the $^{31}P\{^1H\}$ NMR spectrum is resolved into an AX pattern with $J(P_A{-}P_X) = 306$ Hz. The large J value indicates that these phosphorus nuclei are mutually trans. For these to be inequivalent, there must now (−85 °C) be slow rotation about the Ru–P bonds *and* the favored conformer must lack a mirror plane of symmetry (**4**). The crowding implied by this

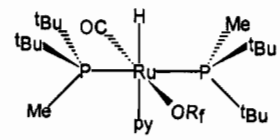

4

observation is supported by the fact that, already at −65 °C, the pyridine ring hydrogens show five distinct chemical shifts. There is thus no rotation about the Ru–N bond. This is consistent with a flat pyridine ring being sandwiched between the alkyl substituents of two bulky phosphines.

Just as for pyridine, nitriles (acetonitrile, acrylonitrile)[30] bind reversibly to $RuHX(CO)P_2$ species. Room-temperature ^1H NMR spectra of $RuHX(CO)P_2$ (X = I, Cl, F) containing 0.5 or 2.0 equiv of RCN show one set of nitrile signals indicating rapid reversible nitrile binding. In contrast to the pyridine case, $RuHI(CO)P_2$ shows no evidence for phosphine replacement by MeCN, even in the presence of 5 equiv of MeCN. This reflects the less sterically demanding nature of the slender MeCN ligand.

(28) Both the 1.2 equiv MeOH and 10 equiv MeOH solutions show (at 25 °C) ν_{CO} at 1902 cm^{-1}, which argues against coordination of the methanol oxygen to ruthenium at 25 °C.

(29) Brothers, P. *J. Prog. Inorg. Chem.* **1981**, *28*, 1. See also ref 1c.

(30) Upon addition of acrylonitrile to $RuHX(CO)P_2$ (X = I, Cl, F), ^1H NMR reveals that the olefinic proton resonances have shifted downfield from that of neat acrylonitrile. This is inconsistent with binding of the olefin functionality.

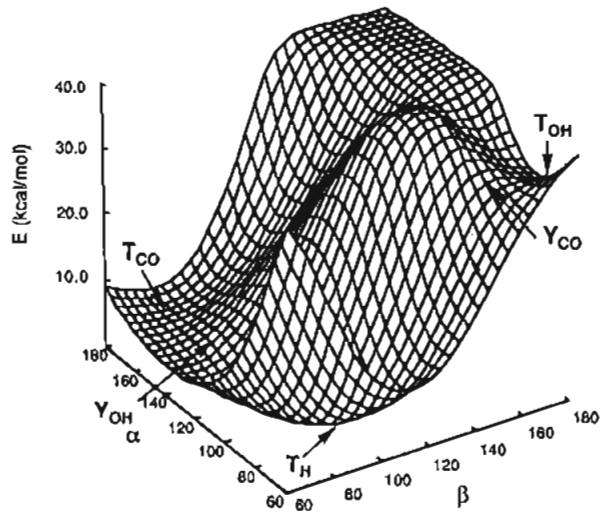

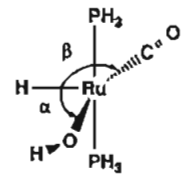

	E(kcal/mol)
T_H	0.
T_{CO}	6.2
Y_{OH}	8.4
T_{OH}	29.4
Y_{CO}	35.9

Figure 2. EHT potential energy surface (PES), $E = f(\alpha,\beta)$, for RuH(OH)(CO)$(PH_3)_2$. The Ru–P bonds are perpendicular to the RuH(OH)(CO) plane. Key: T_H ($\alpha = 90°$, $\beta = 90°$), T_{CO} ($\alpha = 180°$, $\beta = 90°$), T_{OH} ($\alpha = 90°$, $\beta = 180°$), and Y_{OH} ($\alpha = 140°$, $\beta = 80°$). The OH bond is kept in the RuH(CO) plane.

Overall, then, the ground state of $RuHX(CO)P_2$ species is not unsaturated ("16-electron count"), but the molecules nevertheless react like Lewis acids, albeit highly sterically encumbered ones.

Origin of the Metal Coordination Geometry. It has been shown that a diamagnetic d^6 ML_5 complex distorts away from the Jahn–Teller active trigonal bipyramidal structure.[31] Two more stable structures are possible: a square pyramid (also called T) and a distorted trigonal bipyramid[32] (also called Y). Theoretical studies[12,33] have shown that the T and Y structures are very close in energy and that the preference for one over the other comes from a subtle balance of σ and π properties of the ligands.

In our systems, the exceptional bulk of the two phosphine ligands justifies the assumption that these be mutually trans. Our study will therefore focus on the three non-phosphine ligands constrained to a mirror plane perpendicular to the P–Ru–P direction. The term T_L (respectively Y_L) will designate a geometrical arrangement in which L is the foot of the T (respectively Y).

The previous theoretical studies have shown that a T_D structure **5** with the strongest σ-donor D at the foot of the T, (i.e., trans to the empty site) is preferred in case of three pure σ-donor ligands. The presence of a π-acceptor ligand also makes the T structure more stable. When one of the ligands is a π-donor X, a Y_X structure **6** with X at the foot of the Y is observed. It was shown that this structure permits the formation of a partial π bond between the empty metal d orbital and the lone pair of X. No such π bond is present in the T structure since all symmetry-adapted d orbitals are filled. This partial M–X multiple bond stabilizes Y over T.

The mixed case (one π-donor and one π-acceptor ligand, as in $RuHX(CO)P_2$) is therefore an especially interesting case since opposite influences are at work. From our present experimental

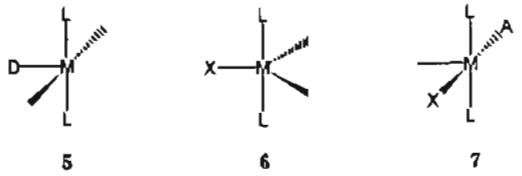

results, the T structure in which the π-donor X ligand and the π-acceptor A ligand are trans to each other (**7**) is more stable. An earlier qualitative analysis yielded the following explanation of this structure preference.[4] In a T structure, which is a fragment of an octahedron, the nonbonding orbital(s) is (are) destabilized by the lone pair(s) of X (a single- or double-faced π-donor group). The π-acceptor ligand can diminish this destabilization by means of back-donation into its empty π^* orbitals. For best stabilization, the two ligands should be *trans* to each other, yielding a "push-pull" effect (**8**). This interaction should transfer electrons from the Ru–X region into the empty π^*_{CO}, which should lower the CO stretching frequency. As it will appear later, the CO stretching is also influenced by the nature of the Ru–X σ bond.

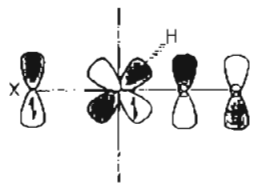

8

In order to quantify this analysis, we have calculated the potential energy surface (PES) for RuH(OH)(CO)$(PH_3)_2$ (EHT) and also for $RuHCl(CO)(PH_3)_2$ (*ab initio*). Both calculations show a preference for a T shape with the π-donor X and π-acceptor ligands *trans* to each other (**7**).

(a) EHT Study of RuH(OH)(CO)$(PH_3)_2$. The calculated PES $E = f(\alpha,\beta)$ with constraints described in the Experimental Section (Figure 2) shows a global minimum for $\alpha = 92°$ and $\beta = 90°$, which corresponds to the nearly square-pyramidal structure T_H (**9**), very close to the experimental one. A secondary minimum T_{OH} (**10**) ($\alpha = 90°$ and $\beta = 180°$), considerably higher in energy (29.4 kcal/mol), can be disregarded. One notes that T_H is located in a rather flat valley containing Y_{OH} (**11**) (8.4 kcal/mol above T_H) and T_{CO} (**12**) (6.2 kcal/mol above T_H). None of these structures are real minima on the PES. However, the presence of this flat valley indicates that the complex should be fluxional.

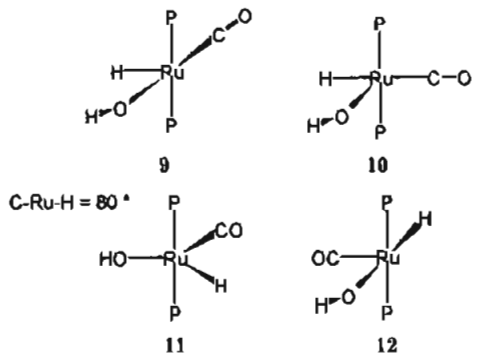

It is worth noting that the ^{t}Bu groups in P^tBu_2Me are of limited utility as diastereotopic reporters of precisely this fluxionality in molecules of the class $MXYZ(P^tBu_2Me)_2$. This is because site exchange among isomers **13–15** by bending in the plane of these five atoms never generates a time-average mirror plane containing the M–P bond. Only if **13** goes rapidly to **13′** will the time-average mirror plane be generated to make the two ^{t}Bu groups on a single phosphorus equivalent. In fact, the compounds

(31) Burdett, J. K.; Perutz, R. N.; Poliakoff, M.; Turner, J. J. *J. Chem. Soc., Chem. Commun.* **1975**, 157.
(32) Werner, H.; Hohn, A.; Dziallas, M. *Angew. Chem., Int. Ed. Engl.* **1986**, *25*, 1090. Fryzuk, M. D.; MacNeil, P. A.; Boll, R. G. *J. Am. Chem. Soc.* **1986**, *108*, 6414. Fryzuk, M. D.; MacNeil, P. A.; Massey, R. L.; Boll, R. G. *J. Organomet. Chem.* **1989**, *328*, 231. Harlow, R. L.; Thorn, D. L.; Baker, R. T.; Jones, N. L. *Inorg. Chem.* **1992**, *31*, 993.
(33) Rachidi, E.-I.; Eisenstein, O.; Jean, Y. *New. J. Chem.* **1990**, *14*, 671.

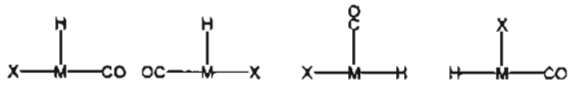

13′ (T_H) (T_{CO}) (T_X)

13 **14** **15**

reported here show two ^{t}Bu chemical shifts, so the **13** → **13′** conversion is slow, if it occurs at all.

We will now discuss the relative energies of several important structures on the PES. The origin of the high energy of T_{OH} has been previously described.[33] Three structures appear to be close in energy T_H (**9**), T_{CO} (**12**), and Y_{OH} (**11**). The higher energy of Y_{OH} relative to T_H comes, in part, from the interaction between the occupied orbitals of the two proximate ligands (CO and H).[33]

Two structures remain to be compared: T_H and T_{CO}. Although difficult to estimate, it is reasonable to believe that the Ru–H and Ru–C(O) σ interactions are similar in both complexes since CO and H are both good σ-donor ligands. The π interactions thus distinguish the two structures.

(i) For T_H. The *yz* and *xy* orbitals are destabilized by the two oxygen lone pairs with *yz* being more so because it interacts with a pure p orbital of the OH ligand. The *xz* orbital remains nonbonding. The two vacant π^*_{CO} orbitals are well positioned to stabilize *yz* (**16**) and *xy* (**17a**) as already mentioned.

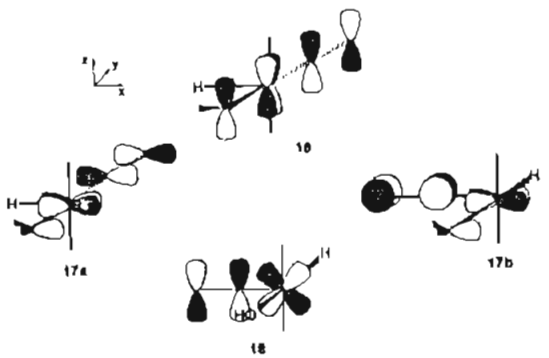

17a **16** **17b** **18**

(ii) For T_{CO}. The destabilization of *yz* and *xy* is similar to that in T_H but the CO does not have such a good stabilizing effect in this case. Thus, $(\pi^*_{CO})^x$ (i.e., parallel to the *y* axis) can stabilize *xy* (**17b**) but $(\pi^*_{CO})^z$ lacks the proper symmetry to interact with *yz*. Instead, it stabilizes very weakly the already more stable *xz* orbital (**18**). Therefore, in this last structure, some of the destabilization which originates from the interaction of the orbitals of the π-donating ligand and the occupied orbitals of the metal has not been diminished by the electron withdrawing group. *There are two push–pull interactions in T_H, but only one in T_{CO}.* A trans arrangement of the two ligands is thus best to alleviate the four-electron repulsion.

(b) *Ab Initio* PES of $RuHCl(CO)(PH_3)_2$. Figure 3 gives the potential energy surface at the HF level of $RuHCl(CO)(PH_3)_2$ with the same geometrical constraints as in the EHT PES. It is strikingly similar to the EHT PES for $RuH(OH)(CO)(PH_3)_2$. There is a global minimum at $\alpha = 105.6°$ and $\beta = 83.6°$, which corresponds to the nearly square-pyramidal structure T_H, very close to the structure found experimentally for $RuH(OSiPh_3)(CO)(P^tBu_2Me)_2$. The T_{Cl} structure, $\alpha = 94.7°$ and $\beta = 163.9°$, is found as a secondary minimum at higher energies (26.8 kcal/mol above T_H from the PES; 19.7 kcal/mol after optimization), with a Y_{CO} transition state (from the PES approximately 38 kcal/mol above T_H) interconnecting the two minima. Furthermore, the two other possible structures (Y_{Cl} and T_{CO}) are located in a low energy valley with energies of 5.1 and 6.8 kcal/mol, respectively, above T_H, but are not stationary points. As expected,[12,33] the nearly trigonal-bipyramidal structure lies at a very high energy. The two minima, T_H and T_{Cl}, have been further fully optimized and MP2 calculations have been carried out on

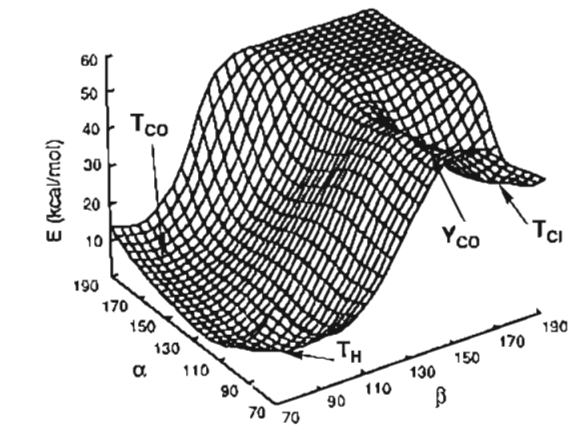

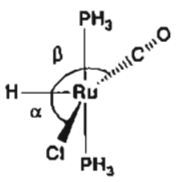

	E(kcal/mol)	
	PES	Optimized
T_H	0.	0.
T_{CO}	6.8	–
T_{Cl}	26.8	19.69
Y_{CO}	38.1	–

Figure 3. HF *ab initio* PES, $E = f(\alpha,\beta)$, for $RuHCl(CO)(PH_3)_2$. The Ru–P bonds are perpendicular to the RuHCl(CO) plane. Key: T_H ($\alpha = 105.6°$, $\beta = 83.6°$), T_{CO} ($\alpha = 180°$, $\beta = 90°$), T_{Cl} ($\alpha = 94.7°$, $\beta = 163.9°$), and Y_{Cl} ($\alpha = 140°$, $\beta = 80°$).

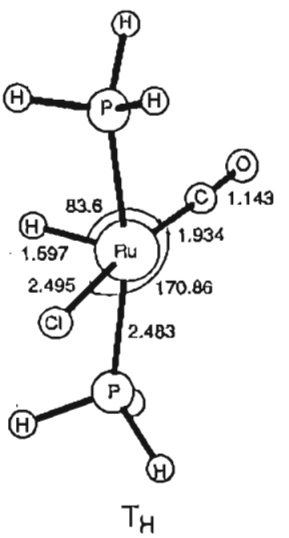

T_H

Figure 4. HF optimized structure for $RuHCl(CO)(PH_3)_2$.

the optimized structures. Selected structural parameters of T_H are given in Figure 4.

Bonding and Structure with Variation in the Group X. The preceding results establish clearly the generality of the finding that a T structure with the donor and acceptor ligands in a trans arrangement is preferred. We will now turn our attention to the detailed structure and properties associated with the change in the ligand X.

The total energies of the fully optimized structures of the model complexes $RuHX(CO)(PH_3)_2$ (X = F, Cl, OH, OCH_3, $OSiH_3$) at both the HF and the MP2/HF level are given in the supplementary material, and the most important geometrical parameters are given in Table 4, where the experimental values for the complex $RuH(OSiPh_3)(CO)(P^tBu_2Me)_2$, are also given for comparison.

The calculated structure of the complexes is in good agreement with the experimental data available. All complexes adopt the T_H structure. The CO ligand is nearly collinear with the Ru–X bond in all cases. Furthermore, the two Ru–P bonds are always almost perpendicular to the mirror plane, with a small bending

Table 4. Selected Calculated Geometrical Parameters of the *ab Initio* Optimized Structures of $RuHX(CO)(PH_3)_2$[a]

	X = Cl	X = F	X = $OSiH_3$	X = OH	X = OCH_3	X = $OSiPh_3$[b]
Ru–C	1.934	1.936	1.936	1.943	1.948	1.819/1.800
	1.806	*1.843*	*1.813*	*1.823*	*1.823*	
Ru–X	2.495	2.041	2.052	2.042	2.037	2.057/2.057
Ru–H	1.597	1.588	1.589	1.592	1.595	
Ru–P	2.483	2.484	2.485	2.482	2.484	2.374/2.389
C–O	1.143	1.145	1.146	1.146	1.146	1.160/1.172
	1.226	*1.226*	*1.227*	*1.228*	*1.229*	
X–R			1.600	0.946	1.400	1.584/1.588
C–Ru–X	170.86	170.49	170.36	171.03	171.87	163.87/166.42
P–Ru–P	167.47	163.79	166.38	164.59	166.34	175.00/177.27
Ru–X–R			167.09	132.63	135.31	168.8/162.21

[a] All distances are given in Å, and angles are given in deg. The Ru–C and C–O values in italics are those obtained after partial optimization at the MP2 level. [b] Experimental data for the $RuH(CO)(OSiPh_3)(P^tBu_2Me)_2$ complex are given in this column.

away from the carbonyl ligand. The Ru–P bond lengths are essentially independent of the nature of the basal ligands and 0.1 Å longer than in the experimental structure.[34]

The Ru–O and O–Si bond lengths are very well reproduced as is the obtuse angle at the oxygen. The angle at the oxygen is notably larger for SiH_3 than for CH_3 or H. *Ab initio* calculations on R–O–R′ (R, R′ = CH_3, $SiCH_3$) have also shown that the presence of silyl groups increases the angle at the oxygen.[35] This was suggested to be due to π-delocalization of the oxygen lone pairs into the empty π^*_{SiH3} orbitals. However, steric strain, especially in the case of the bulky $SiPh_3$, should also contribute to the enlargement of the oxygen angle. Other Ru–X bond lengths are well reproduced. Thus, the calculated Ru–Cl (2.495 Å) is close to the experimental value in $CpRuCl(PR_3)_2$ (2.453 Å)[36a] and in $CpRuCl(Ph_2PC(H)MeCH_2PPh_2)$ (2.444 Å).[36b] The calculated (2.04 Å) Ru–F bond length is very close to that in $[Ru(CO)_3F_2]_4$ (1.99 Å Ru–F terminal, 2.04 Å Ru–F bridged).[37]

In all cases, the structure with the OR groups lying in the mirror plane of the complex was the more stable but with very low rotation barriers (1.6, 3.9, and 4.6 kcal/mol for R = H, CH_3, and SiH_3, respectively, at the HF level). No electronic factor favors the in-plane orientation of the OR group since the two oxygen lone pairs interact with nearly degenerate d orbitals. Thus, the preferred orientation must be due to steric factors.

It is well known that back-donation is poorly represented at the HF level. For this reason and in consideration of the size of the complexes, we have done a partial optimization of the Ru–C and C–O bond lengths at the MP2 level while keeping all the other variables at the value found at the HF level. The results are also given in Table 4. The Ru–C bond length is well reproduced but the C–O length is longer than the experimental one. This is to be expected since the distance of free CO at this level of theory is 1.138 Å (HF) and 1.189 Å (MP2), compared to the experimental value of 1.128 Å.[38] Therefore, we will discuss only *trends* in calculated values, which should have greater validity. Calculations show (Table 4) that the CO bond length varies little with the nature of X. However, the CO distance is shorter in the case of chloride than in the case of alkoxide which is a first indication of a lower stretching frequency for alkoxide ligands.

CO Stretching Frequencies. Since ν_{CO} values are the traditional way to assess electron availability in a metal carbonyl compound,

Table 5. Calculated C–O Vibrational Frequencies (cm^{-1}) for $RuHX(CO)(PH_3)_2$[a]

X	calcd model 1[c]	calcd model 2[d]	exptl
Cl	1688	1717	1904
F	1678	1714	1892
OH	1684	1715	1896
OCH_3	1676	1710	1885
$OSiH_3$	1672	1710	1886[b]
free CO	1901		2143

[a] The phosphine ligands in all the experimental complexes are P^tBu_2Me. [b] Frequency for the $RuH(CO)(OSiMe_3)(P^tBu_2Me)_2$ complex. [c] Model 1 for the vibration. [d] Model 2 for the vibration **19**.

the X-dependence of ν_{CO} reported here represents an attractive observable for comparison to theory. In particular, we want to understand the surprising trend down the group of halides. Two approximate models were used here for the CO stretching mode. Since the CO stretching mode is isolated from the other vibrational modes,[39] we can use a model (model 1) in which the CO bond length varies by Δ_{CO} while all other structural parameters (notably Ru–C) stay at their optimal values **19**. We have also used another

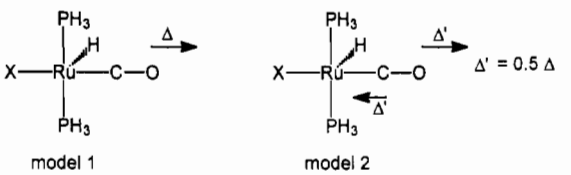

19

model (model 2) in which C and O each move in opposite directions by $0.5\Delta_{CO}$ (**19**). The calculated frequencies (Table 5) with both models are far from the experimental ones. However, at our level of calculations, the stretching frequency of free CO is 2265 cm^{-1} (HF) and 1901 cm^{-1} (MP2) compared to the experimental 2143 cm^{-1}.[38] Taking into account the difference between calculated and experimental values,[40] the MP2 values with model 2 are closer to the experimental results. However, the most important result is that both models for the CO vibration give the same trend as a function of X. The frequency decreases in the order Cl, OH, F, $OSiH_3$, and OCH_3, which is in excellent agreement with the experimental determination. In order to understand the origin of this variation, we have examined the electronic distribution in this series of molecules using the Mulliken charges and overlap population. A full description is given in the supplementary material. We give here a summary of the results.

From the Mulliken analysis, the Ru–F and Ru–O bonds are strongly ionic while Ru–Cl has a significant covalent character. The ionic character is primarily in the σ(Ru–X) bond. There are only small variations in the C–O overlap population although it is overall larger in the case of halide than in the alkoxides. The π donation of F and Cl are found to be similar. The energy levels of the three filled d Ru orbitals reflect the electron-donating ability of X (Figure 5). They agree with the qualitative picture (**16**–**18**) with *xz* being the lowest in energy and *xy* and *yz* being higher due to the influence of the X lone pairs. These last two orbitals are higher in energy for an alkoxy than for a halide group. They are the highest in the case of OCH_3. Metal charge also influences the d orbital energy. The positive charge of Ru bonded to F, without compensatory F→Ru π donation, yields low-lying d orbital energies.

What then, is the origin of the variation in ν_{CO}? Either a rise[41] or a fall[42] in ν_{CO} has been observed depending on the nature of the metal center bonded to the CO ligand. Electrostatic interaction (like in $CuCO^+$) raises the CO vibration frequency.[43]

(34) Such differences can originate from both the use of model PH_3 ligands, and the neglect of electron correlation effects.
(35) Shambayati, S.; Blake, J. F.; Wierschke, S. G.; Jorgensen, W. L.; Schreiber, S. L. *J. Am. Chem. Soc.* **1990**, *112*, 697.
(36) (a) Bruce, M. I.; Wong, F. S.; Skelton, B. W.; White, A. H. *J. Chem. Soc., Dalton Trans.* **1981**, 1398. (b) Morandini, F.; Consiglio, G.; Straub, B.; Ciani, G.; Sironi, A. *J. Chem. Soc., Dalton Trans.* **1983**, 2293.
(37) Marshall, C. J.; Peacock, R. D.; Russel, D. R.; Wilson, I. L. *J. Chem. Soc., Chem. Commun.* **1970**, 1643.
(38) Herzberg, G.; Huber, K. P. *Molecular Spectra and Molecular Structure*; Constants of Diatomic Molecules 4; Van Nostrand Reinhold: New York, 1979.
(39) The band assigned ν_{CO} in $RuHCl(CO)P_2$ shifts <1 cm^{-1} in $RuDCl(CO)P_2$. This proves that there is no significant mixing of RuH and CO stretching modes.
(40) The ν_{CO} values should be shifted up by 240 cm^{-1} (MP2) with model 2.

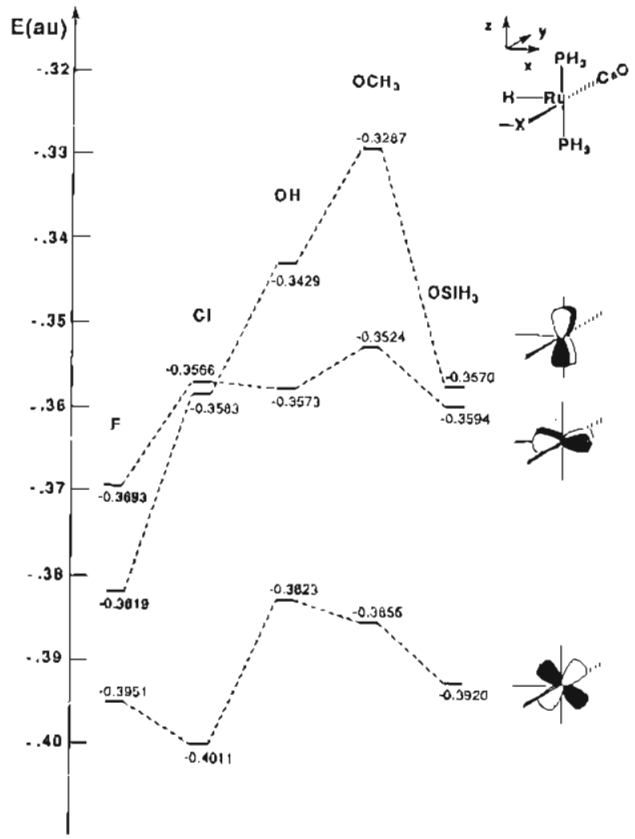

Figure 5. *Ab initio* energy levels of the occupied d orbitals of RuHX(CO)(PH$_3$)$_2$ (X = F, Cl, OH, OCH$_3$, OSiH$_3$).

This has been attributed to the loss of electrons out of the HOMO (5σ) of CO.[44] In contrast, the back-donation into π^*_{CO} lowers the frequency (e.g., NiCO).[34] Exchange effects have also been suggested.[44b] In our case, we have clear evidence for the π effect. Thus, alkoxides, which are significantly better π donors than halides, lower ν_{CO} the most. The comparison F/Cl is more difficult to explain. A study by Fenske and Hall[45] has suggested that F may be a better π donor than Cl in octahedral 18-electron complexes on the basis of significant difference in the d_π/p_π interactions. Our π-stabilized–unsaturated case seems to be different since there is little difference in the π donation between the two halides. The overlap integral is larger for the short Ru–F bond and compensates (in part) for the deeper energy of the fluorine orbitals. The large difference between the two halides in our calculations lies in the ionicity of the two bonds, Ru–F being more ionic than Ru–Cl. This means that the electrostatic interaction between the metal and CO should be larger in the case of F leading to *higher* frequency and not *lower* as experimentally observed. It must be that changes in lower bonding C/O σ orbitals contribute significantly to the overall trend down the halide group in addition to that in the weakly bonding 5σ. This may be a consequence of the low-lying orbital energy of an electron-deficient metal center. One can now understand the influence of the entire halide series by a monotonic extrapolation: the ionicity of the Ru–X bond should decrease in the order F, Cl, Br, and I while the π-donating effect should vary less. Thus, the CO vibration should appear at higher frequency in the order F < Cl < Br < I as indeed experimentally observed. Similar reasons account for the higher frequency for SPh compared to OPh.[46,47]

The σ and π effects vary in a different way as one moves along a row or down a column of the periodic table. Moving along a row from group 17 to group 15 corresponds to large increase in the π-donating power of the X lone pair(s). In contrast, moving down a column has less effect on the π system since the increase in the Ru–X bond length (decrease overlap) diminishes the donating power of higher energy orbital. The increase of the ionicity of the Ru–X going up the periodic table dominates over the π-effect and (for RuHX(CO)P$_2$ compounds) lowers the CO frequency. The fact that fluoride differs so dramatically (cf. ν_{CO}) from all the other halides suggests that a systematic study of the reactivity of π-stabilized unsaturated fluoro compounds may prove fruitful.

Acknowledgment. We thank E. R. Davidson for helpful discussions and F. B. C. Machado for providing a plot of the CO 5σ orbital. This work was supported by the U.S. National Science Foundation and the French CNRS under Grants CHE-9103915 and INT-88-14838, respectively. We thank the Indiana University Institute for Advanced Study for support of the visit of O.E., Johnson Matthey/Aesar for material support, and Scott Haubrich for a sample of [LiOB(Mes)$_2$(OEt$_2$)]$_2$ and for useful discussions. Laboratoire de Chimie Théorique is associated with the CNRS (URA 506) and is a member of ICMO and IPCM. M.P.S. thanks the University of Thessaloniki and the CNRS for financing his stay at Orsay.

Supplementary Material Available: Tables giving full crystallographic details, positional and thermal parameters for RuH(OSiPh$_3$)(CO)(P^{t}Bu$_2$Me)$_2$, Cartesian and internal coordinates of the optimized structures at the HF level and HF and MP2/HF total energy for RuH(X)(CO)(PH$_3$)$_2$ for X = Cl, F, OH, OCH$_3$, OSiH$_3$, Mulliken overlap populations and charges, and complete AO populations, of the HF level structures, a plot of 5σ of CO from *ab initio* calculations, and a drawing of the least-squares fit of the two independent molecules, and text giving a discussion of the CO stretching frequencies in RuHX(CO)(PH$_3$)$_2$ (29 pages). Ordering information is given on any current masthead page.

(41) Beattie, I. R.; Jones, P. J.; Young, N. A. *J. Am. Chem. Soc.* **1992**, *114*, 6146.
(42) This is generally the case in organometallic complexes and in particular in our complexes.
(43) Sodupe, M.; Bauschlicher, C. W.; Lee, T. J. *Chem. Phys. Lett.* **1992**, *189*, 266.
(44) (a) A plot of 5σ from *ab initio* calculations with basis set from Kunze and Davidson (Kunze, K. L.; Davidson, E. R. *J. Phys. Chem.* **1992**, *96*, 2129) shows that this orbital is weakly CO bonding (see supplementary material). In addition, the orbital which describes the metal–CO σ bond in Cr(CO)$_6$ is also CO bonding. This contrasts with the currently accepted idea that 5σ is CO antibonding (Elschenbroich, C.; Salzer, A. *Organometallics*, VCH: New York, **1989**, p 227). It is thus unclear how 5σ by *itself* will increase the CO vibration frequency. (b) Pacchioni, G.; Minewa, T.; Bogus, D. *Surf. Sci.* **1992**, *275*, 450.
(45) Hall, M. B.; Fenske, R. D. *Inorg. Chem.* **1972**, *11*, 1619. See also Bursten, B. F.; Green, M. R. *Prog. Inorg. Chem.* **1988**, *36*, 393.
(46) The structural consequence of thiolate π-donation has been thoughtfully analyzed. See: Ashby, M. T. *Comments Inorg. Chem.* **1990**, *10*, 297.
(47) The high ν_{CO} value (1902 cm^{-1}) observed in RuH$_2$(CO)(py)P$_2$ is consistent with the covalent nature of the Ru–H bond and the absence of a π-donating effect for the hydride. It also shows why authentic 16-valence electron hydride compounds are almost never isolable.